

Robustness of Clocks to Input Noise

Michele Monti,¹ David K. Lubensky,² and Pieter Rein ten Wolde¹

¹*FOM Institute AMOLF, Science Park 104, 1098 XE Amsterdam, Netherlands*

²*Department of Physics, University of Michigan, Ann Arbor, Michigan 48109-1040, USA*



(Received 18 September 2017; revised manuscript received 30 March 2018; published 14 August 2018)

To estimate the time, many organisms, ranging from cyanobacteria to animals, employ a circadian clock which is based on a limit-cycle oscillator that can tick autonomously with a nearly 24 h period. Yet, a limit-cycle oscillator is not essential for knowing the time, as exemplified by bacteria that possess an “hourglass”: a system that when forced by an oscillatory light input exhibits robust oscillations from which the organism can infer the time, but that in the absence of driving relaxes to a stable fixed point. Here, using models of the Kai system of cyanobacteria, we compare a limit-cycle oscillator with two hourglass models, one that without driving relaxes exponentially and one that does so in an oscillatory fashion. In the limit of low input noise, all three systems are equally informative on time, yet in the regime of high input-noise the limit-cycle oscillator is far superior. The same behavior is found in the Stuart-Landau model, indicating that our result is universal.

DOI: [10.1103/PhysRevLett.121.078101](https://doi.org/10.1103/PhysRevLett.121.078101)

Many organisms, ranging from animals, plants, insects, to even bacteria, possess a circadian clock, which is a biochemical oscillator that can tick autonomously with a nearly 24 h period. Competition experiments on cyanobacteria have demonstrated that these clocks can confer a fitness benefit to organisms that live in a rhythmic environment with a 24 h period [1,2]. Clocks enable organisms to estimate the time of day, allowing them to anticipate, rather than respond to, the daily changes in the environment. While it is clear that circadian clocks which are entrained to their environment make it possible to estimate the time, it is far less obvious that they are the only or best means to do so [3,4]. The oscillatory environmental input could, for example, also be used to drive a system which in the absence of any driving would relax to a stable fixed point rather than exhibit a limit cycle. The driving would then generate oscillations from which the organism could infer the time. It thus remains an open question what the benefits of circadian clocks are in estimating the time of day.

This question is highlighted by the timekeeping mechanisms of prokaryotes. While circadian clocks are ubiquitous in eukaryotes, the only known prokaryotes to possess circadian clocks are cyanobacteria, which exhibit photosynthesis. The best characterized clock is that of the cyanobacterium *Synechococcus elongatus*, which consists of three proteins, KaiA, KaiB, and KaiC [5]. The central clock component is KaiC, which forms a hexamer that is phosphorylated and dephosphorylated in a cyclical fashion under the influence of KaiA and KaiB. This phosphorylation cycle can be reconstituted in the test tube, forming a bona fide circadian clock that ticks autonomously in the absence of any oscillatory driving with a period of nearly 24 h [6]. However, *S. elongatus* is not the only cyanobacterial species. *Prochlorococcus marinus* possesses *kaiB*

and *kaiC*, but lacks (functional) KaiA. Interestingly, this species exhibits daily rhythms in gene expression under light-dark (LD) cycles but not in constant conditions [7,8]. Recently, Johnson and co-workers made similar observations for the purple bacterium *Rhodospseudomonas palustris*, which harbors homologs of KaiB and KaiC. Its growth rate depends on the KaiC homolog in LD but not constant conditions [4], suggesting that the bacterium uses its Kai system to keep time. Moreover, this species too does not exhibit sustained rhythms in constant conditions, but does show daily rhythms in, e.g., nitrogen fixation in cyclic conditions. *P. marinus* and *R. palustris* thus appear to keep time via an “hourglass” mechanism that relies on oscillatory driving [4,7,8]. These observations raise the question of why some bacterial species like *S. elongatus* have evolved a bona fide clock that can run freely, while others have evolved an hourglass timekeeping system.

Troein *et al.* studied the evolution of timekeeping systems in silico [9]. They found that only in the presence of seasonal variations and stochastic fluctuations in the input signal did systems evolve that can also oscillate autonomously. However, organisms near the equator have evolved self-sustained oscillations [4], showing that seasonal variations cannot be essential. Pfeuty *et al.* suggest that limit-cycle oscillators have evolved because they enable timekeepers that ignore the uninformative light-intensity fluctuations during the day (corresponding to a dead zone in the phase-response curve), yet selectively respond to the more informative intensity changes around dawn and dusk [10].

Here, we hypothesize that the optimal design of the readout system that maximizes the reliability by which cells can estimate the time depends on the noise in the input signal. To test this idea, we study three different network designs from which the cell can infer time (Fig. 1). (i) A

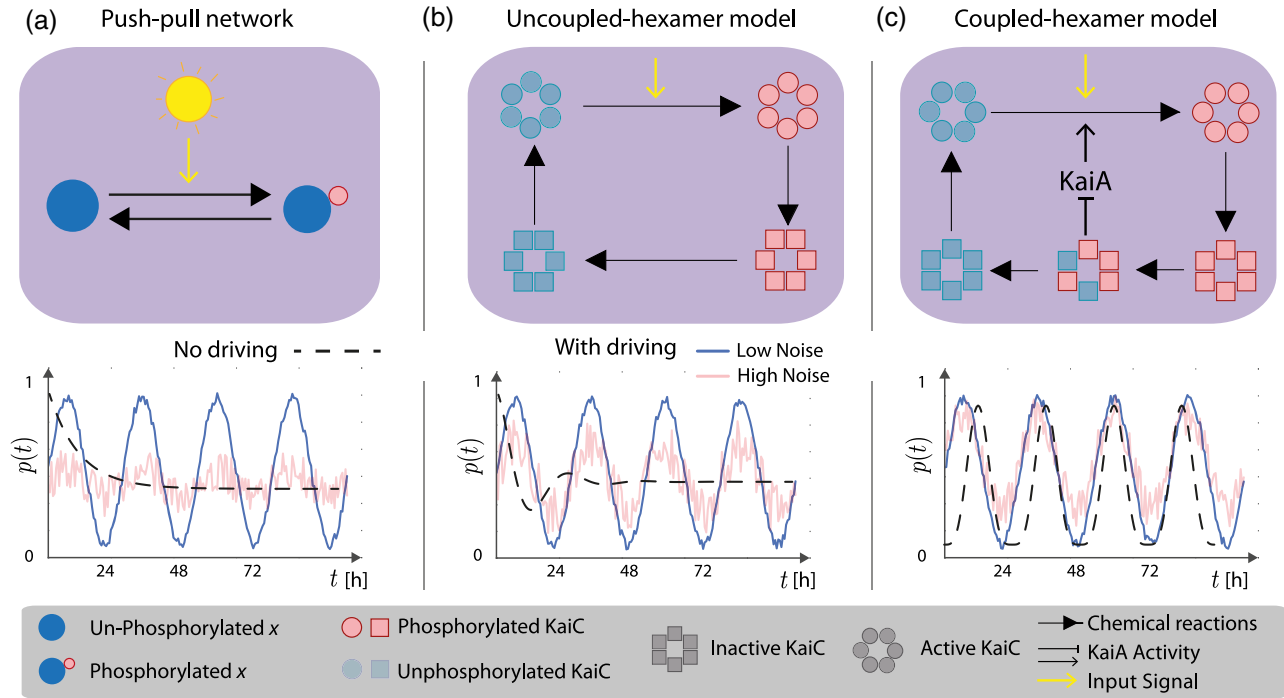


FIG. 1. Overview of different timekeeping systems. (a) A push-pull network (PPN). Each protein can switch between a phosphorylated and an unphosphorylated state, and the input signal enhances the phosphorylation rate. In the absence of driving, the PPN relaxes exponentially to a steady state (middle panel). Yet, in the presence of an oscillatory input, e.g., sunlight, the system exhibits oscillations from which the time can be inferred (lower panel). (b) The uncoupled-hexamer model (UHM), inspired by the Kai system of *P. marinus*. It consists of KaiC hexamers which can switch between an active state in which the phosphorylation level tends to rise and an inactive one in which it tends to fall. The phosphorylation rate is, via changes in the ATP/ADP ratio, enhanced by the light input [11,12]. The system is akin to a harmonic oscillator, with an intrinsic frequency ω_0 , resulting from the hexamer phosphorylation cycle. However, the hexamers are not coupled via KaiA as in the CHM shown in panel (c), so it cannot sustain autonomous oscillations; in the absence of driving, it relaxes in an oscillatory fashion to a stable fixed point (middle panel). (c) The coupled-hexamer model (CHM), inspired by the Kai system of *S. elongatus*. Like the UHM, it consists of KaiC hexamers, which tend to be phosphorylated cyclically. However, in contrast to the UHM, the hexamers are synchronized via KaiA, such that the system can exhibit limit-cycle oscillations in the absence of driving (middle panel). In all models, time is estimated from the protein phosphorylation fraction $p(t)$.

simple push-pull network (PPN), in which a readout protein switches between a phosphorylated and an unphosphorylated state [Fig. 1(a)]. Because the phosphorylation rate increases with the light intensity, the phosphorylation level oscillates in the presence of oscillatory driving, enabling the cell to estimate the time. This network lacks an intrinsic oscillation frequency, and in the absence of driving it relaxes to a stable fixed point in an exponential fashion. (ii) An uncoupled hexamer model (UHM), which is inspired by the Kai system of *P. marinus* [Fig. 1(b)]. This model consists of KaiC hexamers which each have an inherent propensity to proceed through a phosphorylation cycle. However, the phosphorylation cycles of the hexamers are not coupled among each other, and without a common forcing the cycles will therefore desynchronize, leading to the loss of macroscopic oscillations. In contrast to the proteins of the PPN, each hexamer is a tiny oscillator with an intrinsic frequency ω_0 , which means that an ensemble of hexamers that has been synchronized initially, will, in the absence of driving, relax to its fixed point in an oscillatory manner. (iii) A coupled hexamer model (CHM),

which is inspired by the Kai system of *S. elongatus* [Fig. 1(c)]. As in the previous UHM, each KaiC hexamer has an intrinsic capacity to proceed through a phosphorylation cycle, but, in contrast to that system, the cycles of the hexamers are coupled and synchronized via KaiA, as described further below. Consequently, this system exhibits a limit cycle, yielding macroscopic oscillations with intrinsic frequency ω_0 even in the absence of any driving.

Here we are interested in the question how the precision of time estimation is limited by the noise in the input signal, and how this limit depends on the architecture of the readout system. We thus focus on the regime in which the input noise dominates over the internal noise [13] and model the different systems using mean-field (deterministic) chemical rate equations. In Ref. [14], we also consider internal noise, and show that, at least for *S. elongatus*, the input-noise dominated regime is the relevant limit.

The chemical rate equation of the PPN is $\dot{x}_p = k_f s(t)[x_T - x_p(t)] - k_b x_p(t)$, where $x_p(t)$ is the concentration of phosphorylated protein, x_T is the total concentration, $k_f s(t)$ is the phosphorylation rate k_f times the input signal

$s(t)$, and k_b is the dephosphorylation rate. The uncoupled (UHM) and coupled (CHM) hexamer model are based on the Kai system [32–39]. In both models, KaiC switches between an active conformation in which the phosphorylation level tends to rise and an inactive one in which it tends to fall [32,37]. Experiments indicate that the main Zeitgeber is the ATP/ADP ratio [11,12], meaning the clock predominantly couples to the input $s(t)$ during the phosphorylation phase of the oscillations [11,39]. In both the UHM and the CHM, $s(t)$ therefore modulates the phosphorylation rate of active KaiC. The principal difference between the UHM and CHM is KaiA: (functional) KaiA is absent in *P. marinus* and hence in the UHM [7,8]. In contrast, in *S. elongatus* and hence the CHM, KaiA phosphorylates active KaiC, yet inactive KaiC can bind and sequester KaiA. This gives rise to the synchronization mechanism of differential affinity [14,32,33]. In all three models, the input is modeled as a sinusoidal signal with mean \bar{s} and driving frequency $\omega = 2\pi/T$ plus additive noise $\eta_s(t)$: $s(t) = \sin(\omega t) + \bar{s} + \eta_s(t)$. The noise is uncorrelated with the mean signal, and has strength σ_s^2 and correlation time τ_c , $\langle \eta_s(t)\eta_s(t') \rangle = \sigma_s^2 e^{-|t-t'|/\tau_c}$. A detailed description of the models is given in the Supplemental Material [14].

As a performance measure for the accuracy of estimating time, we use the mutual information $I(p;t)$ between the time t and the phosphorylation level $p(t)$ [13,40]:

$$I(p;t) = \int_0^T dt \int_0^1 dp P(p,t) \log_2 \frac{P(p,t)}{P(p)P(t)}. \quad (1)$$

Here $P(p,t)$ is the joint probability distribution while $P(p)$ and $P(t) = 1/T$ are the marginal distributions of p and t . The quantity $2^{I(p;t)}$ corresponds to the number of time points that can be inferred uniquely from $p(t)$; $I(p;t) = 1$ bit means that from $p(t)$ the cell can reliably distinguish between day and night [41]. The distributions are obtained from running long simulations of the chemical rate equations of the different models [14].

For each system, to maximize the mutual information we first optimized over all parameters except the coupling strength. For the CHM, the coupling strength ρ was taken to be comparable to that of *S. elongatus* [14], and for the PPN and the UHM ρ was set to an arbitrary low value, because in the relevant weak-coupling regime the mutual information is independent of ρ , as elucidated below and in Ref. [14]. For the PPN, there exists an optimal response time $\tau_r \sim 1/k_b$ that maximizes $I(p;t)$, arising from a trade-off between maximizing the amplitude of $p(t)$, which increases with decreasing τ_r , and minimizing the noise in $p(t)$, which decreases with increasing τ_r because of time averaging [14,42]. Similarly, for the UHM, there exists an optimal intrinsic frequency ω_0 of the individual hexamers. The UHM is linear and similar to a harmonic oscillator. Analyzing this system shows that while the amplitude A of the output $x(t)$ is maximized at resonance, $\omega_0 \rightarrow \omega$, the standard deviation σ_x of x is maximized when $\omega_0 \rightarrow 0$, such

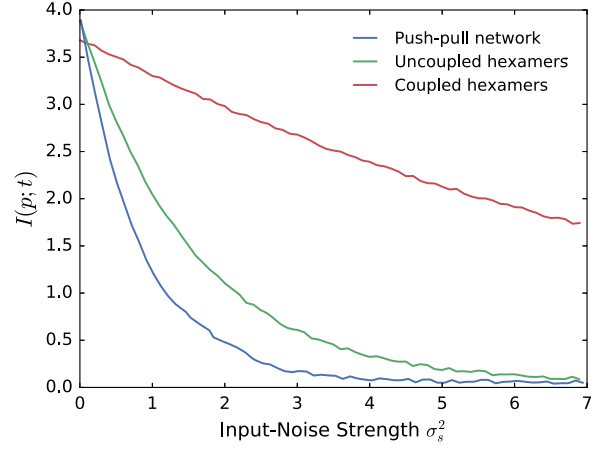


FIG. 2. The mutual information $I(p;t)$ as a function of the input-noise strength σ_s^2 , for the push-pull network, the uncoupled-hexamer model, and the coupled-hexamer model, see Fig. 1. In the limit of low input noise, all systems are equally informative on time, but in the high-noise regime the CHM is most accurate. The parameters have been optimized to maximize $I(p;t)$; since these are (nearly) independent of σ_s^2 (Figs. S1–S3 [14]), they are fixed (Table S1 [14]).

that the signal-to-noise ratio A/σ_x peaks for $\omega_0 > \omega$ [14]. Interestingly, also the CHM exhibits a maximum in A/σ_x for intrinsic frequencies that are slightly off-resonance [14].

Figure 2 shows the mutual information $I(p;t)$ as a function of the input-noise strength σ_s^2 for the three systems. In the regime that σ_s^2 is small, $I(p;t)$ is essentially the same for all systems. However, the figure also shows that as σ_s^2 rises, $I(p;t)$ of the UHM and especially the PPN decrease very rapidly, while that of the CHM falls much more slowly. For $\sigma_s^2 \approx 3$, $I(p;t)$ of the CHM is still above 2 bits, while $I(p;t)$ of the PPN and UHM have already dropped below 1 bit, meaning the cell would no longer be able to distinguish between day and night. Indeed, this figure shows that in the regime of high input noise, a bona fide clock that can tick autonomously is a much better time keeper than a system which relies on oscillatory driving to show oscillations. This is the principal result of our Letter. It is observed for other values of τ_c and other types of input, such as a truncated sinusoid corresponding to no driving at night (Fig. S6 [14]).

The robustness of our observation that bona fide clocks are more reliable timekeepers, suggests it is a universal phenomenon, independent of the details of the system. We therefore analyzed a generic minimal model, the Stuart-Landau model. It allows us to study how the capacity to infer time changes as a system is altered from a damped (nearly) linear oscillator, which has a characteristic frequency but cannot sustain oscillations in the absence of driving, to a nonlinear oscillator that can sustain autonomous oscillations [14]. Near a Hopf bifurcation where a limit cycle appears the effect of the nonlinearity is weak, so that the solution $x(t)$ is close to that of a harmonic

oscillator, $x(t) = 1/2[A(t)e^{i\omega t} + \text{c.c.}]$, where $A(t)$ is a complex amplitude that can be time dependent [43]. The dynamics of $A(t)$ is then given by

$$\dot{A} = -i\nu A + \alpha A - \beta|A|^2 A - \epsilon E, \quad (2)$$

where $\nu \equiv (\omega^2 - \omega_0^2)/(2\omega)$ with ω_0 the intrinsic frequency, α and β govern the linear and nonlinear growth and decay of oscillations, E is the first harmonic of $s(t)$, and $\epsilon \equiv \rho/(2\omega)$ is the coupling strength. Equation (2) gives a universal description of a driven weakly nonlinear oscillator near a supercritical Hopf bifurcation [43].

The nondriven system exhibits a Hopf bifurcation at $\alpha = 0$. By varying α we can thus change the system from a *damped oscillator* ($\alpha < 0$) which in the absence of driving exhibits oscillations that decay, to a *limit-cycle oscillator* ($\alpha > 0$) that shows free-running oscillations. The driven damped oscillator ($\alpha < 0$) always has one stable fixed point with $|A| > 0$ corresponding to sinusoidal oscillations that are synchronized with the driving. The driven limit-cycle oscillator ($\alpha > 0$), however, can exhibit several distinct dynamical regimes [43]. Here, we limit ourselves to the case of perfect synchronization, where $x(t)$ has a constant amplitude A and phase shift with respect to $s(t)$.

To compute $I(x, t)$, we use an approach inspired by the linear-noise approximation [13]. It assumes $P(x|t)$ is a Gaussian distribution with variance $\sigma_x^2(t)$ centered at the deterministic solution $x(t) = 1/2(Ae^{i\omega t} + \text{c.c.})$, where A is obtained by solving Eq. (2) in steady state. To find σ_x^2 , we first compute σ_A^2 from Eq. (2) by adding Gaussian white noise of strength σ_s^2 to E and expanding A to linear order around its fixed point; $\sigma_x^2(t)$ is then obtained from σ_A^2 via a coordinate transformation [14].

Figure 3 shows the mutual information $I(x; t)$ as a function α , for different values of σ_s^2 . The figure shows that $I(x; t)$ rises as the system is changed from a damped oscillator ($\alpha < 0$) to a self-sustained oscillator ($\alpha > 0$). Moreover, the increase is most pronounced when the input noise σ_s^2 is large. The Stuart-Landau model can thus reproduce the qualitative behavior of our computational models, indicating that our principal result is generic. Interestingly, for the parameter set chosen, the CHM is even more robust than the Stuart-Landau model, perhaps because the latter is only weakly nonlinear [14].

To understand why limit-cycle oscillators are more robust to input noise, we study in section SIIE [14] analytical models valid in the limit of weak coupling. For a damped oscillator with a fixed-point attractor (PPN and UHM), we find that the amplitude A of the harmonic oscillations (the signal) increases with the coupling strength ρ , $A \sim \rho$. The noise in the output signal σ_x scales with ρ too, $\sigma_x \sim \rho$, because the coupling amplifies not only the input signal, but also the input noise. Hence, the signal-to-noise ratio A/σ_x is independent of ρ : an oscillator based on a fixed-point attractor faces a fundamental trade-off between

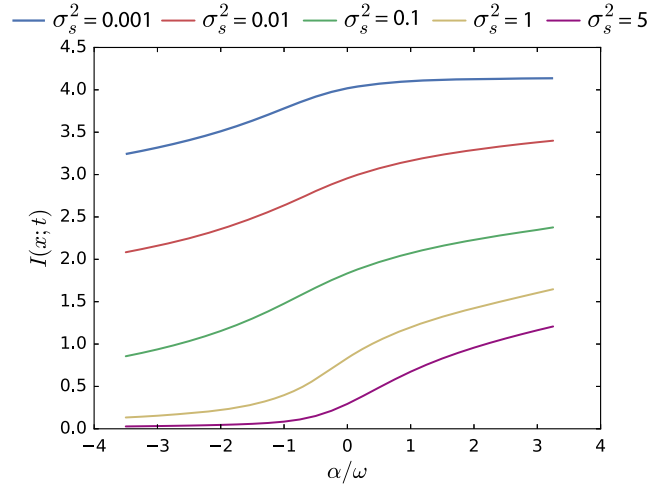


FIG. 3. The mutual information $I(p; t)$ as a function of α of the Stuart-Landau model [Eq. (2)], for different strengths of the input noise σ_s^2 . Clearly, $I(p; t)$ rises as the system is changed from a damped oscillator like the UHM ($\alpha < 0$) to a limit-cycle oscillator like the CHM ($\alpha > 0$). Moreover, the increase is most pronounced when σ_s^2 is large, as also observed for the UHM and CHM, see Fig. 2. Parameters: $\nu = 0$; $\beta = \omega$; $\epsilon = 0.5\omega$; σ_s^2 in units of ω^{-1} .

gain and input noise (section SIIE [14]). A limit-cycle oscillator (CHM) can lift this trade-off: The oscillation amplitude is a robust, intrinsic property of the system, and essentially independent of ρ . The output noise $\sigma_x \sim \sqrt{\rho}$, because the coupling not only amplifies the input noise proportional to ρ , but also generates a restoring force that constrains fluctuations, scaling as $\sim \sqrt{\rho}$ (SIIE [14]). Hence, $A/\sigma_x \sim 1/\sqrt{\rho}$. These scaling arguments show that (i) concerning robustness to input noise, the optimal regime is the weak-coupling regime, and (ii) in this regime, a limit-cycle oscillator is generically more robust to input noise than a damped oscillator. While both oscillators minimize input-noise propagation in this regime, only the limit-cycle oscillator still exhibits a robust amplitude when coupled weakly to the input.

Yet, the coupling cannot be reduced to zero for limit-cycle oscillators. When the intrinsic clock period deviates from 24 h, as it typically will, coupling is essential to phase lock the clock to the driving signal [13]. Moreover, biochemical networks inevitably have some level of internal noise (section SIIF [14]). For the damped oscillator, the output noise σ_x resulting from internal noise is independent of ρ , but since A increases with ρ , $A/\sigma_x \sim \rho$ in the presence of internal noise only: coupling helps to lift the signal above the internal noise. For the limit-cycle oscillator, the restoring force $\sim \sqrt{\rho}$ tames phase diffusion, such that in the presence of only internal noise, the output noise $\sigma_x \sim 1/\sqrt{\rho}$ and $A/\sigma_x \sim \sqrt{\rho}$. Hence, also with regards to internal noise, a limit-cycle oscillator is superior to a damped oscillator in the weak-coupling regime. This analysis also shows,

however, that this regime is not necessarily optimal, since with only internal noise present A/σ_x increases with ρ . In fact, it predicts that in the strong-coupling regime the damped oscillator outperforms the limit-cycle oscillator. We emphasize, however, that in this regime our weak-coupling analysis breaks down and other effects come into play; for example, nonlinearities arising from the bounded character of $p(t)$ distort the signal, reducing information transmission.

In the presence of both noise sources, we expect an optimal coupling that maximizes information transmission (SIIF [14]). For the limit-cycle oscillator the optimum arises from the trade-off between minimizing input-noise propagation and maximizing internal-noise suppression. For the damped oscillator, A/σ_x first rises with ρ because coupling helps to lift the signal above the internal noise, but then plateaus when the input noise (which increases with ρ) dominates over the internal noise; for even higher ρ , it decreases again because of signal distortion. In section SIE [14] we verify these predictions for our computational models using stochastic simulations.

Experiments have shown that the clock of *S. elongatus* has a strong temporal stability with a correlation time of several months [44], suggesting that the internal noise is small. Indeed, typical input-noise strengths based on weather data [45] and internal-noise strengths based on protein copy numbers in *S. elongatus* [46] indicate that in the biologically relevant regime, at least for cyanobacteria, input noise dominates over internal noise (Fig. S5 [14]). In this regime, the focus of our Letter, the optimal coupling is weak and limit-cycle oscillators are generically more robust to input noise than damped oscillators.

This work is part of the research programme of the Netherlands Organisation for Scientific Research (NWO) and was performed at AMOLF. D. K. L. acknowledges NSF Grants No. DMR 1056456 and No. PHY 1607611 to the Aspen Center for Physics, where part of this work was completed. We thank Jeroen van Zon and Nils Becker for a critical reading of the manuscript.

Note added in proof.—The study of Ref. [47] independently arrived at the conclusion that clocks based on limit-cycle oscillators are more robust to input noise.

-
- [1] Y. Ouyang, C. R. Andersson, T. Kondo, S. S. Golden, and C. H. Johnson, *Proc. Natl. Acad. Sci. U.S.A.* **95**, 8660 (1998).
 - [2] M. A. Woelfle, Y. Ouyang, K. Phanvijhitsiri, and C. H. Johnson, *Curr. Biol.* **14**, 1481 (2004).
 - [3] T. Roenneberg and M. Meroow, *J. Biol. Rhythms* **17**, 495 (2002).
 - [4] P. Ma, T. Mori, C. Zhao, T. Thiel, and C. H. Johnson, *PLoS Genet.* **12**, e1005922 (2016).
 - [5] M. Ishiura *et al.*, *Science* **281**, 1519 (1998).

- [6] M. Nakajima *et al.*, *Science* **308**, 414 (2005).
- [7] J. Holtzendorff, F. Partensky, D. Mella, J. F. Lennon, W. R. Hess, L. Garczarek, *J. Biol. Rhythms* **23**, 187 (2008).
- [8] E. R. Zinser *et al.*, *PLoS One* **4**, e5135 (2009).
- [9] C. Troein, J. C. W. Locke, M. S. Turner, and A. J. Millar, *Curr. Biol.* **19**, 1961 (2009).
- [10] B. Pfeuty, Q. Thommen, and M. Lefranc, *Biophys. J.* **100**, 2557 (2011).
- [11] M. J. Rust, S. S. Golden, and E. K. O'Shea, *Science* **331**, 220 (2011).
- [12] G. K. Pattanayak, G. Lambert, K. Bernat, and M. J. Rust, *Cell Rep.* **13**, 2362 (2015).
- [13] M. Monti, D. K. Lubensky, and P. R. ten Wolde, *Phys. Rev. E* **97**, 032405 (2018).
- [14] See Supplemental Material at <http://link.aps.org/supplemental/10.1103/PhysRevLett.121.078101>, which includes Refs. [15–31], for details of computational methods and analytic calculations.
- [15] Y. Xu, T. Mori, and C. H. Johnson, *EMBO J.* **19**, 3349 (2000).
- [16] Y. Nakahira, M. Katayama, H. Miyashita, S. Kutsuna, H. Iwasaki, T. Oyama, and T. Kondo, *Proc. Natl. Acad. Sci. U.S.A.* **101**, 881 (2004).
- [17] T. Nishiwaki *et al.*, *Proc. Natl. Acad. Sci. U.S.A.* **101**, 13927 (2004).
- [18] J. Tomita, M. Nakajima, T. Kondo, and H. Iwasaki, *Science* **307**, 251 (2005).
- [19] S. W. Teng, S. Mukherji, J. R. Moffitt, S. de Buyl, and E. K. O'Shea, *Science* **340**, 737 (2013).
- [20] J. Paijmans, M. Bosman, P. R. ten Wolde, and D. K. Lubensky, *Proc. Natl. Acad. Sci. U.S.A.* **113**, 4063 (2016).
- [21] C. Phong, J. S. Markson, C. M. Wilhoite, and M. J. Rust, *Proc. Natl. Acad. Sci. U.S.A.* **110**, 1124 (2013).
- [22] D. T. Gillespie, *J. Phys. Chem.* **81**, 2340 (1977).
- [23] J. Paulsson, *Nature (London)* **427**, 415 (2004).
- [24] S. Tănase-Nicola, P. B. Warren, and P. R. ten Wolde, *Phys. Rev. Lett.* **97**, 068102 (2006).
- [25] C. C. Govern and P. R. ten Wolde, *Phys. Rev. Lett.* **113**, 258102 (2014).
- [26] R. Cheong, A. Rhee, C. J. Wang, I. Nemenman, and A. Levchenko, *Science* **334**, 354 (2011).
- [27] F. Tostevin and P. R. ten Wolde, *Phys. Rev. E* **81**, 061917 (2010).
- [28] J. Guckenheimer and P. J. Holmes, *Nonlinear Oscillations, Dynamical Systems, and Bifurcations of Vector Fields* (Springer, New York, 1983).
- [29] V. S. Anishchenko *et al.*, *Nonlinear Dynamics of Chaotic and Stochastic Systems: Tutorial and Modern Developments* (Springer, New York, 2007).
- [30] P. B. Warren, S. Tănase-Nicola, and P. R. ten Wolde, *J. Chem. Phys.* **125**, 144904 (2006).
- [31] C. W. Gardiner, *Handbook of Stochastic Methods* (Springer-Verlag, Berlin, 1985).
- [32] J. S. van Zon, D. K. Lubensky, P. R. H. Altena, and P. R. ten Wolde, *Proc. Natl. Acad. Sci. U.S.A.* **104**, 7420 (2007).
- [33] M. J. Rust, J. S. Markson, W. S. Lane, D. S. Fisher, and E. K. O'Shea, *Science* **318**, 809 (2007).
- [34] S. Clodong, U. Dühring, L. Kronk, A. Wilde, I. Axmann, H. Herzog, and M. Kollmann, *Mol. Syst. Biol.* **3**, 90 (2007).

- [35] T. Mori, D. R. Williams, M. O. Byrne, X. Qin, M. Egli, H. S. Mchaourab, P. L. Stewart, and C. H. Johnson, *PLoS Biol.* **5**, e93 (2007).
- [36] D. Zwicker, D. K. Lubensky, and P. R. ten Wolde, *Proc. Natl. Acad. Sci. U.S.A.* **107**, 22540 (2010).
- [37] J. Lin, J. Chew, U. Chockanathan, and M. J. Rust, *Proc. Natl. Acad. Sci. U.S.A.* **111**, E3937 (2014).
- [38] J. Paijmans, D. K. Lubensky, and P. R. ten Wolde, *PLoS Comput. Biol.* **13**, e1005415 (2017).
- [39] J. Paijmans, D. K. Lubensky, and P. R. ten Wolde, *Biophys. J.* **113**, 157 (2017).
- [40] M. Monti and P. R. ten Wolde, *Phys. Biol.* **13**, 035005 (2016).
- [41] G. Tkačik and A. M. Walczak, *J. Phys. Condensed Matter* **23**, 153102 (2011).
- [42] N. B. Becker, A. Mugler, and P. R. ten Wolde, *Phys. Rev. Lett.* **115**, 258103 (2015).
- [43] A. Pikovsky, M. Rosenblum, and J. Kurths, *Synchronization: A Universal Concept in Nonlinear Sciences* (Cambridge University Press, Cambridge, England, 2003).
- [44] I. Mihalcescu, W. H. Hsing, and S. Leibler, *Nature (London)* **430**, 81 (2004).
- [45] L. Gu *et al.*, *Agric. For. Meteorol.* **106**, 117 (2001).
- [46] Y. Kitayama, H. Iwasaki, T. Nishiwaki, and T. Kondo, *EMBO J.* **22**, 2127 (2003).
- [47] W. Pittayakanchit *et al.*, eLife (to be published).